3D Extrudable Cellulose-Based Bioink with High Printability, Mechanical Strength, and Biocompatibility

Na Li
Prof. Zhenyu Jason Zhang

Nano-Formulation Engineering group
School of Chemical Engineering
University of Birmingham

TAPPI NANO DIVISION

Background

Restoration of Bone Defect

- Autografts
- Allografts
- **Bone tissue engineered (BTE) Scaffolds**

BTE Scaffolds

- **Components**

1. Cells
2. Growth factors
3. Polymers (artificial extracellular matrix)

- **Fabrication**

1. Phase separation
2. Self-assemble…
3. **3D bioprinting**

Bioprinting Hydrogels (bioinks)

- **Why hydrogels?**

1. Highly hydrated
2. Porous structure
3. Biocompatibility
4. Tunable biodegradability
5. Properly mechanical strength
6. Sustainability

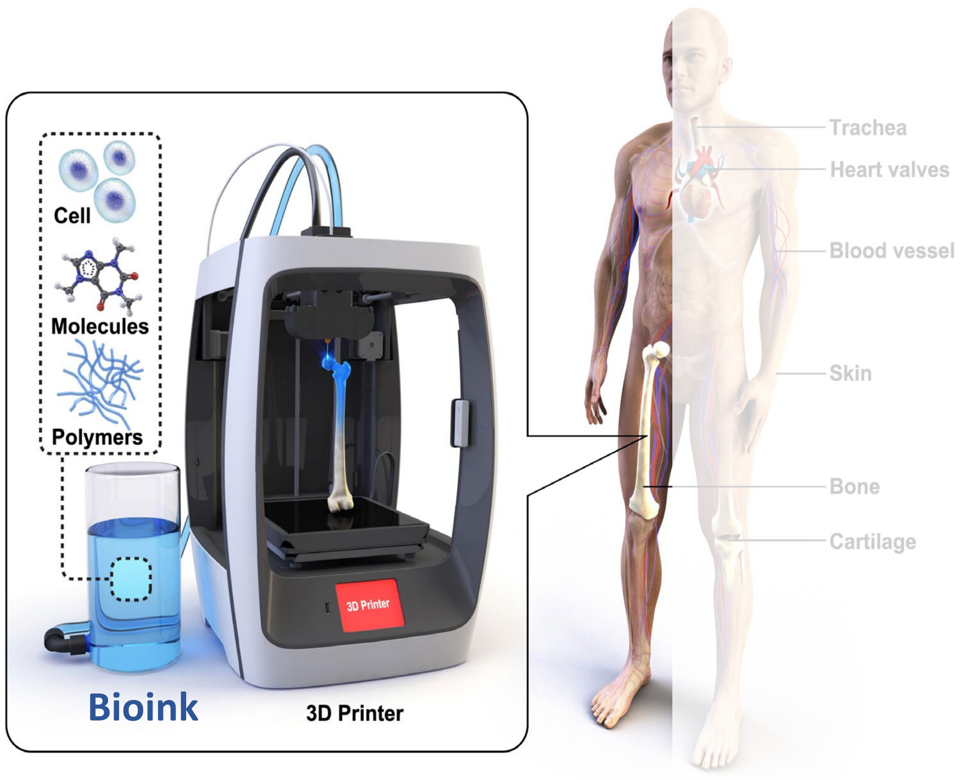

How to design bioinks, mainly the polymer networks, to mimic the functional complexity of native bone tissues maximally

How we do that?

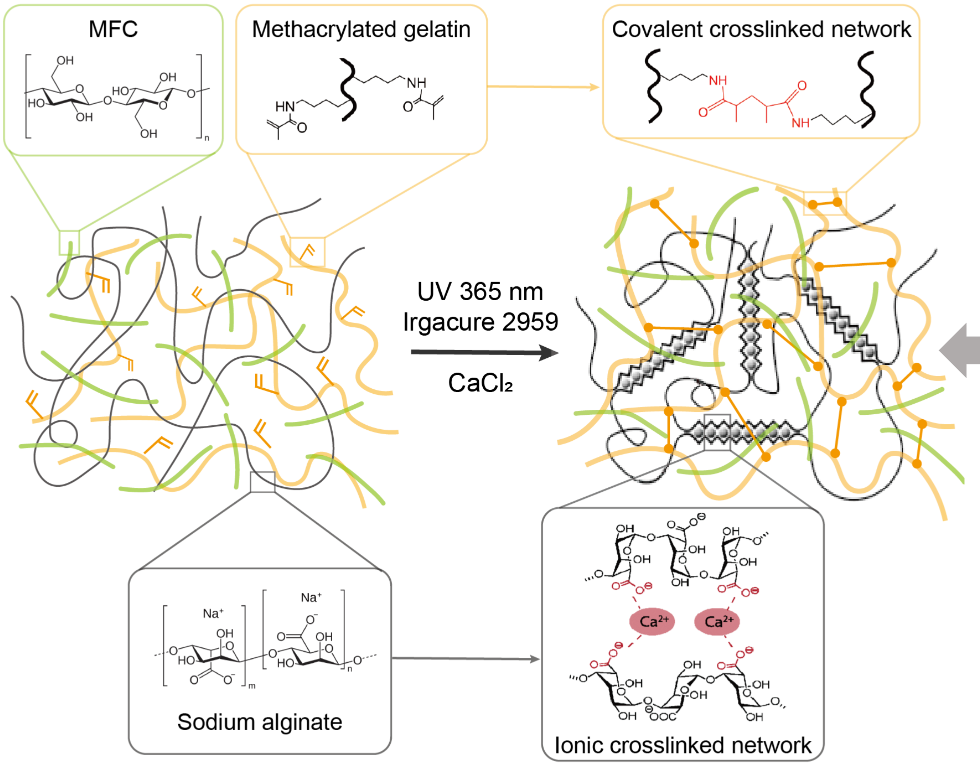

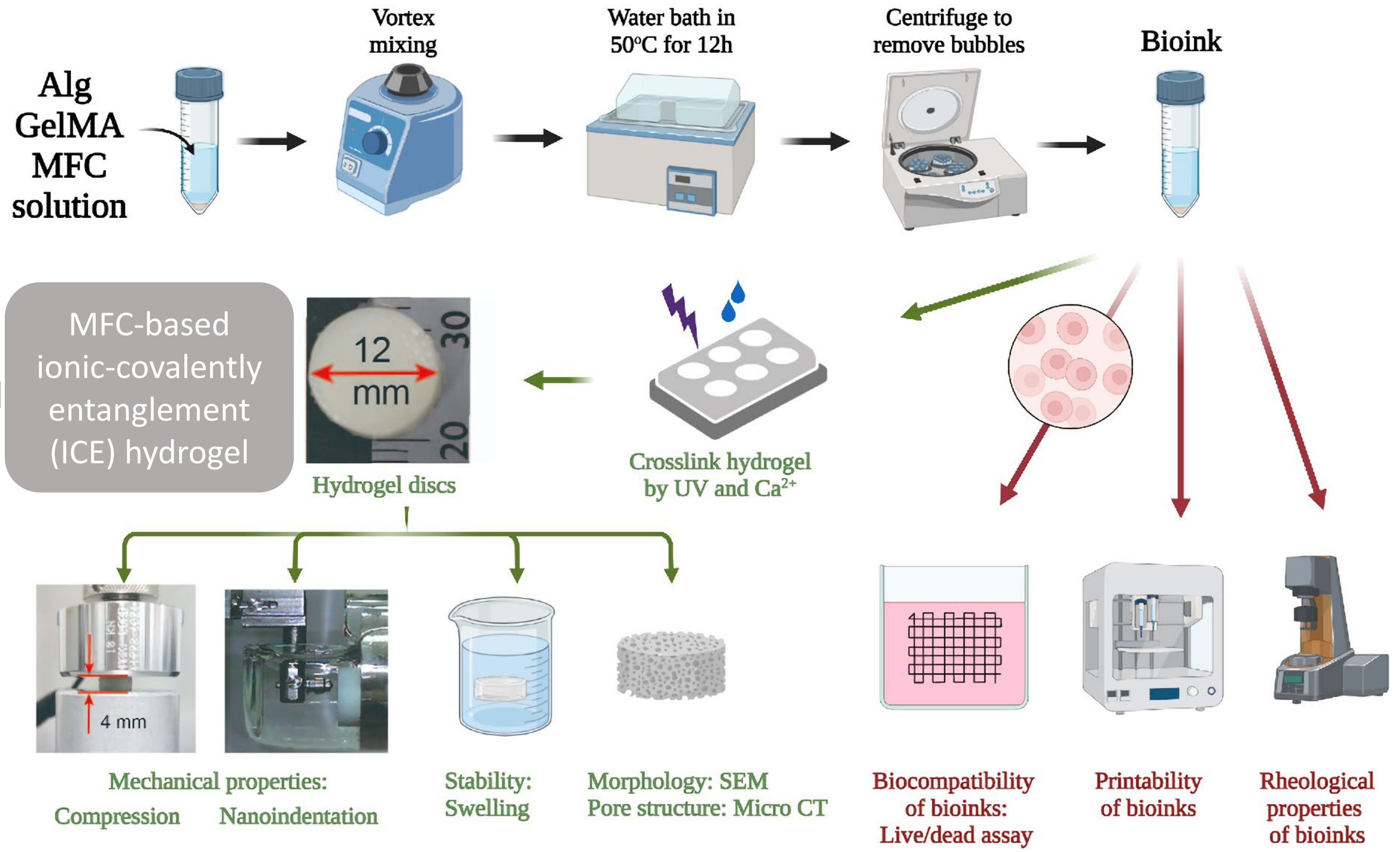

Aim: Develop bioink formulations with high printability during extrusion, excellent mechanical properties after being crosslinked and cytocompatibility after implantation.

Bioinks - What do they look like? Sol/Gel?

After inverting centrifuge tubes for 1 h at RT….

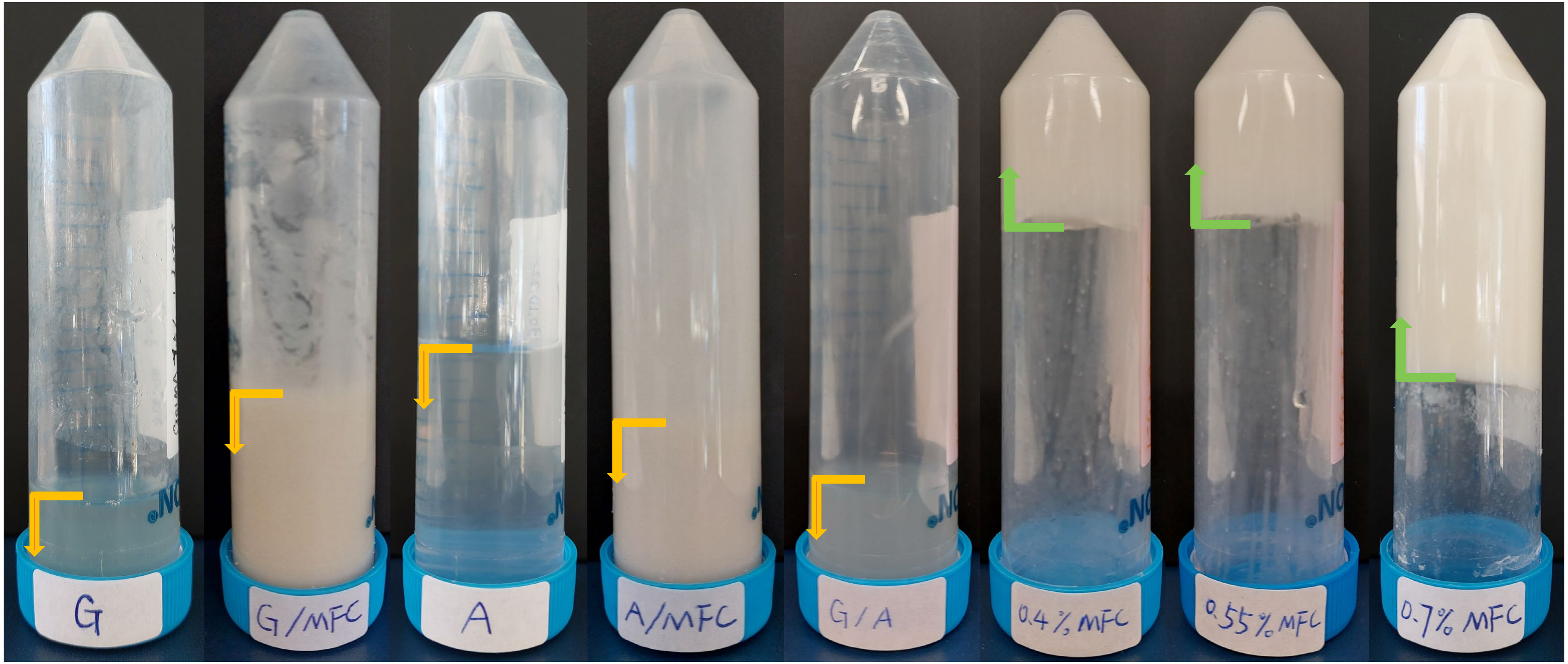

GelMA

GelMA
0.7% MFC

Alginate

Alginate
0.7% MFC

GelMA
Alginate

GelMA
Alginate
0.4% MFC

GelMA
Alginate
0.55% MFC

GelMA
Alginate
0.7% MFC

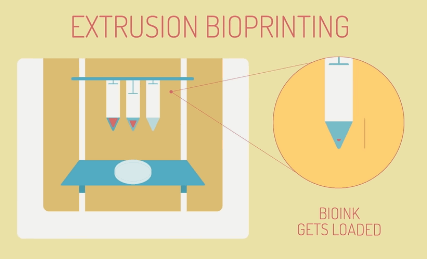

Rheological properties of bioinks

Before printing

Yield Point

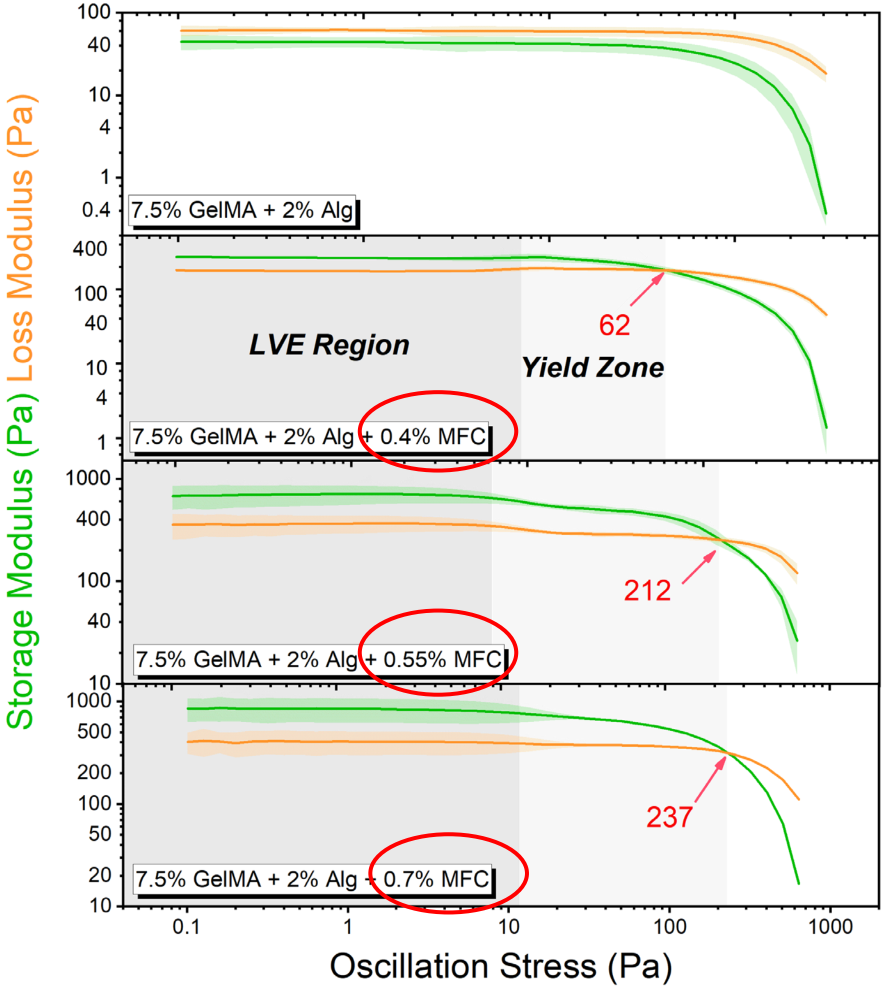

- G’’ > G’
- Always like Sol
- No yield point

- Before yield point: G’ > G’’ gel-like
- After yield point: G’’ > G’ sol-like
- The yield point increased with the increase of MFC in bioink.

Before printing, gel-like MFC-based bioinks can facilitate uniform distribution of components (cells) without deposition

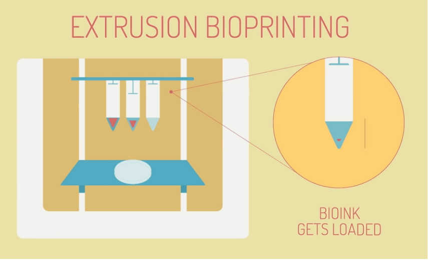

Rheological properties of bioinks

During printing

Shear-thinning (Viscosity decreased with increasing shear rate)

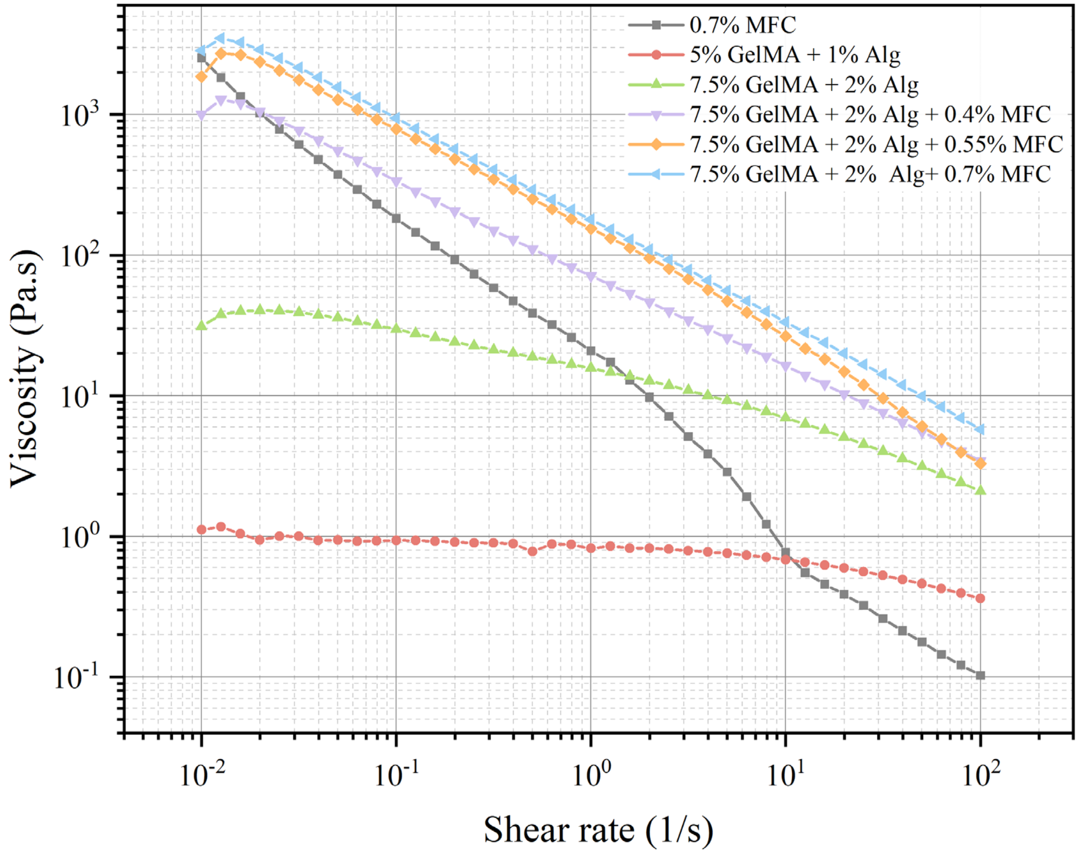

Power-law model ($\tau = K\gamma^n$)	
Samples	Flow index n
0.7% MFC Slurry	**0.02**
5% GelMA + 1% Alg	0.73
7.5% GelMA + 2% Alg	0.52
7.5% GelMA + 2% Alg + 0.4% MFC	**0.34**
7.5% GelMA + 2% Alg + 0.55% MFC	**0.2**
7.5% GelMA + 2% Alg + 0.7% MFC	**0.26**

- Pure MFC had the most excellent shear-thinning behaviour.
- Incorporation of MFC promoted the shear thinning behaviour of the bioink.

MFC can help bioinks smoothly pass through the nozzles of the printer without clogging.

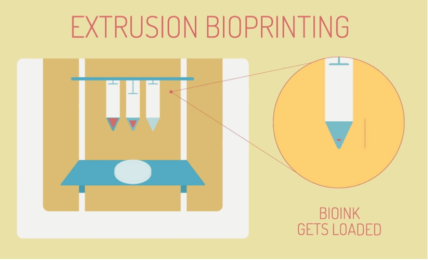

Rheological properties of bioinks

Postprinting

Recoverability

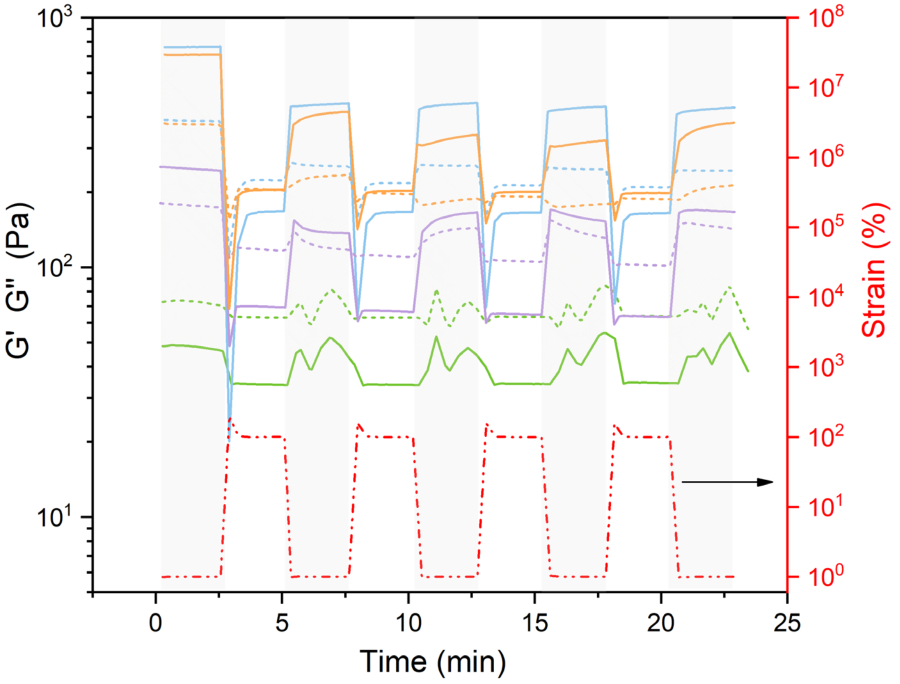

7.5% GelMA + 2% Alg
7.5% GelMA + 2% Alg + 0.4% MFC
7.5% GelMA + 2% Alg + 0.55% MFC
7.5% GelMA + 2% Alg + 0.7% MFC
Strain
Solid lines for G'
Dash lines for G''

- Both of G' and G'' recovered rapidly during 4 large-strain cycles.
- Bioink without MFC: G'' > G'
- Bioinks with MFC
  - High strain (100%): G'' > G' sol-like during printing
  - Low strain (1%): G' > G'' gel-like postprinting

After extrusion, bioinks with MFC can return to a gel state again for layer-by-layer printing.

Printability of Bioinks – Droplets or filaments?

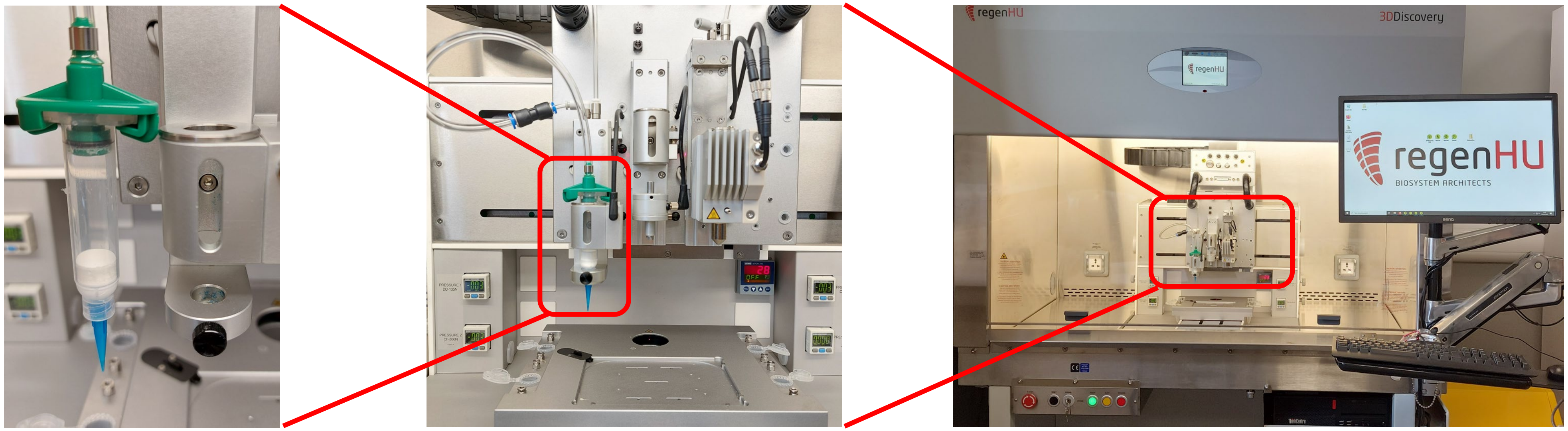

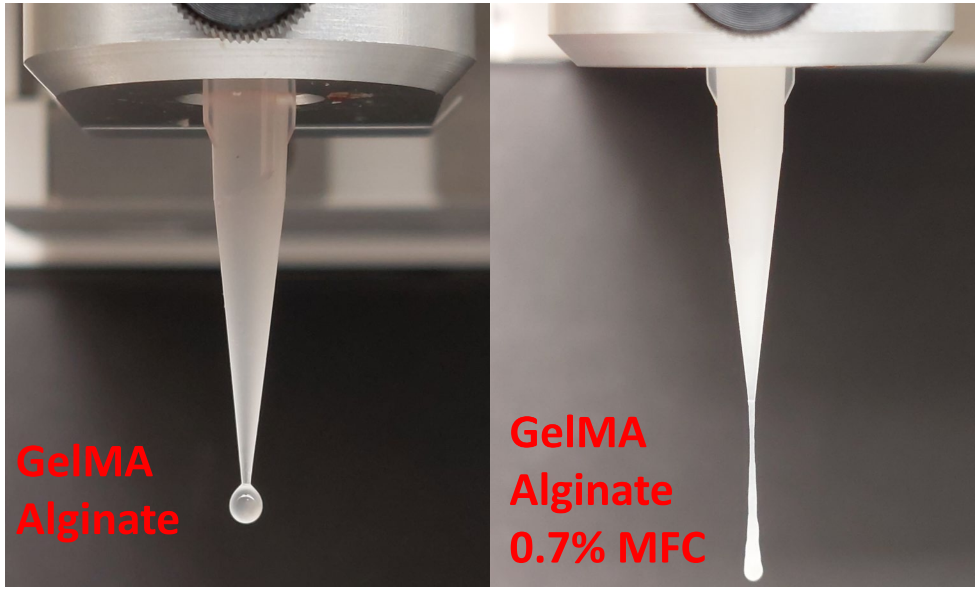

3D Printing Parameter Optimization Index (POI)

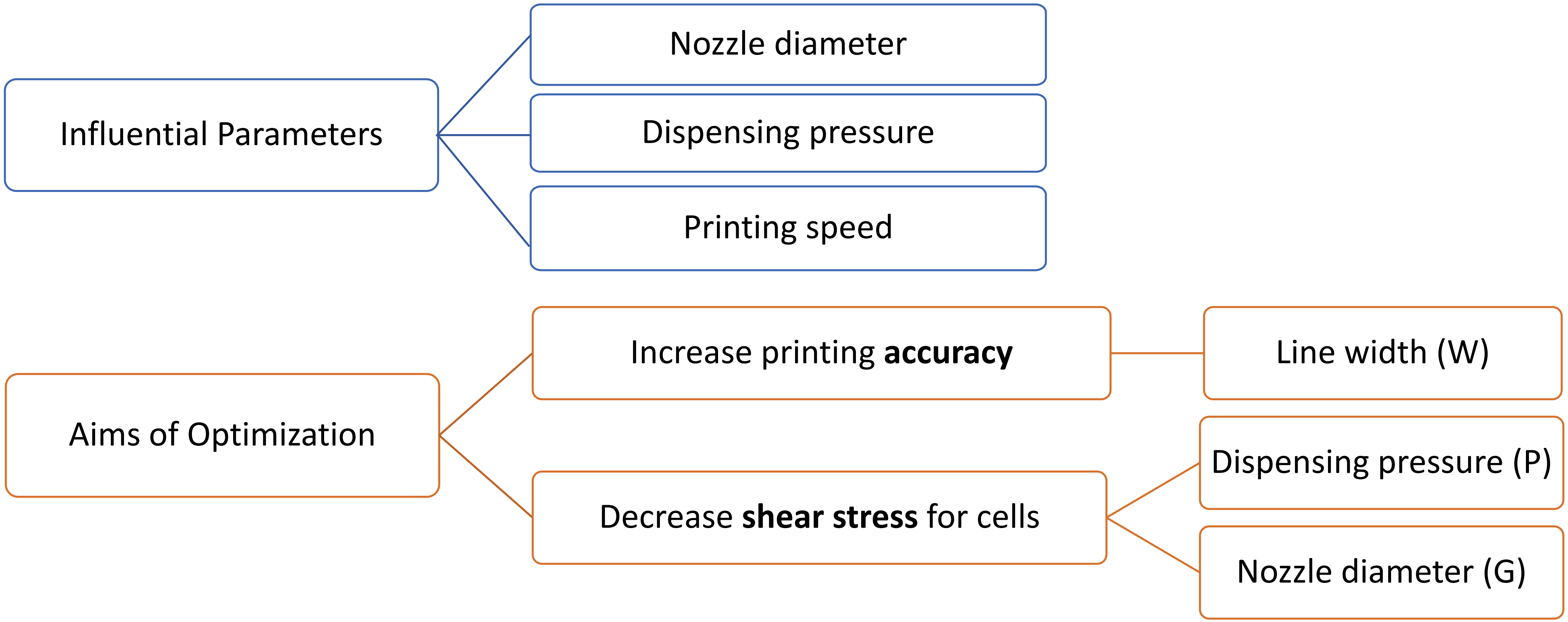

$$POI = \frac{Accuracy}{Shear\ Stress} = \frac{1}{Line\ width} \times \frac{1}{Pressure \cdot Nozzle\ Gauge} = \frac{1}{W \cdot P \cdot G}$$

$$POI_i = \frac{POI}{POI_{max,n}}$$

https://doi.org/10.1016/j.bprint.2017.09.001

3D Printing Parameter Optimization – **27G nozzle (D200um)**

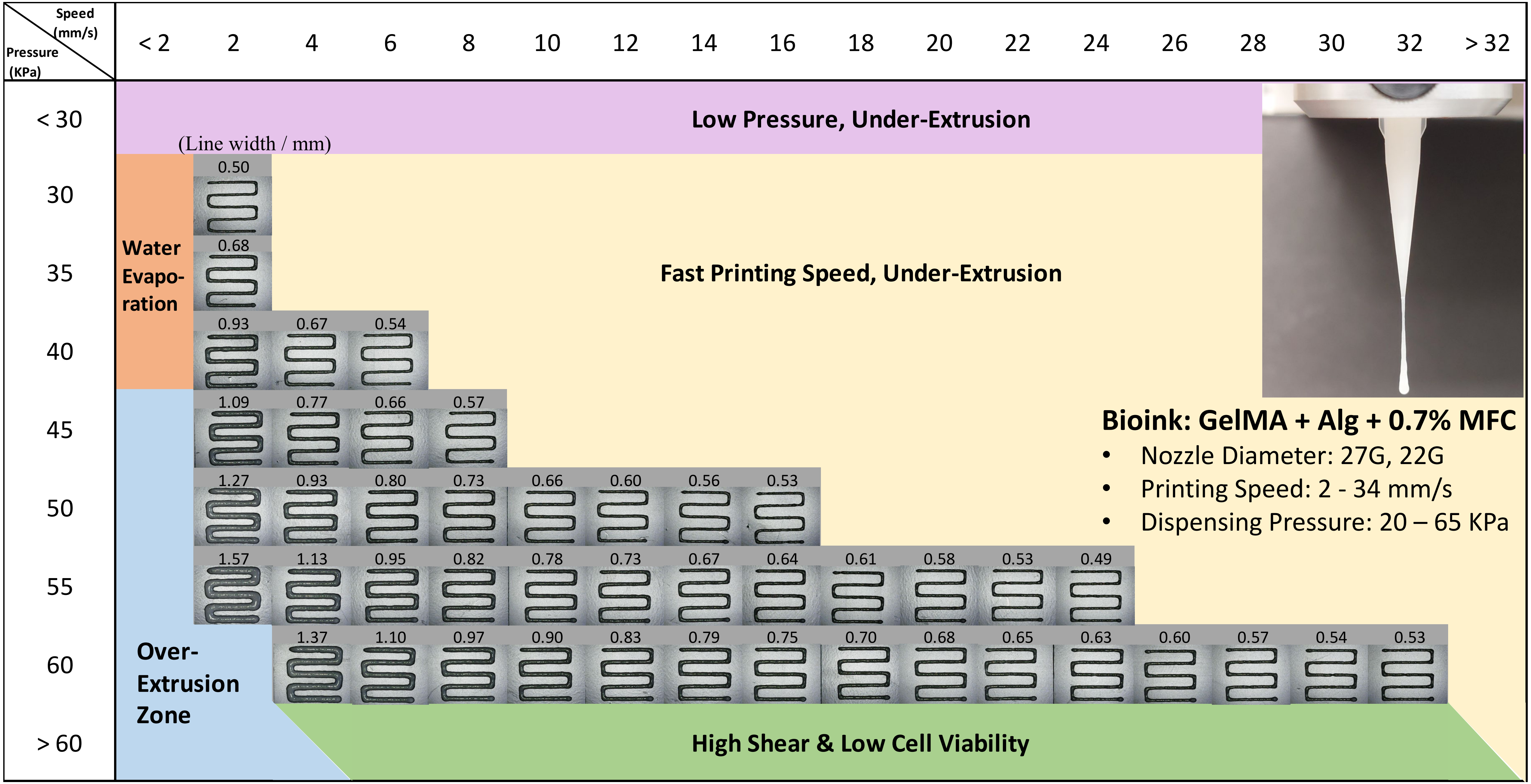

3D Printing Parameter Optimization – **27G nozzle (D200um)**

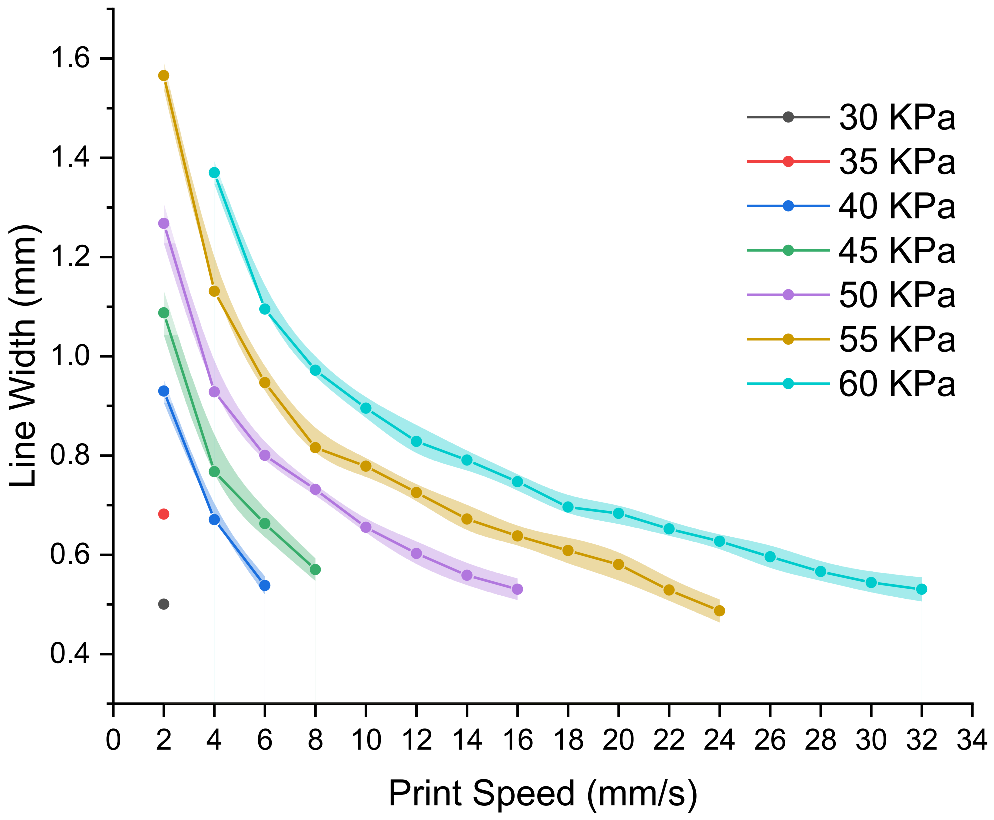

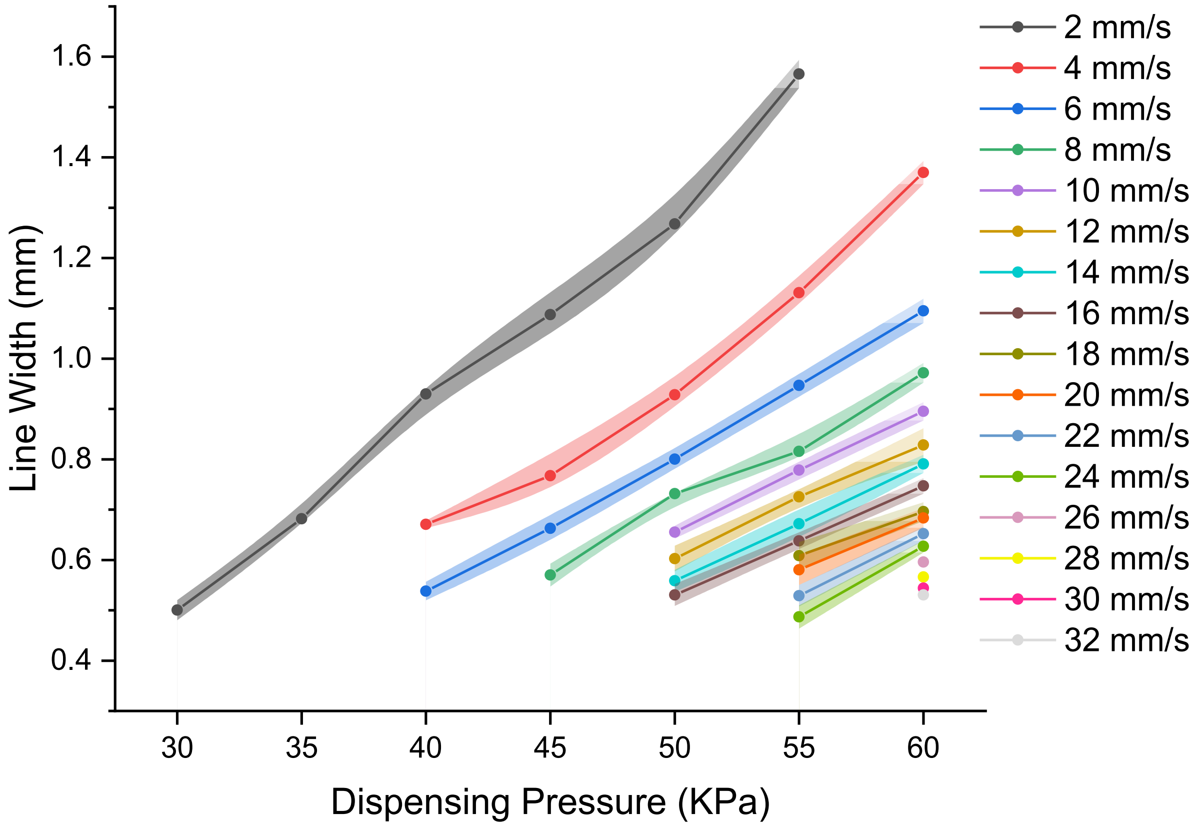

Under the same pressure, the strand width decreased **exponentially** with increasing printing speed.

At the same printing speed, the strand width increased **linearly** with increasing dispensing pressure.

3D Printing Parameter Optimization – **22G nozzle (D410um)**

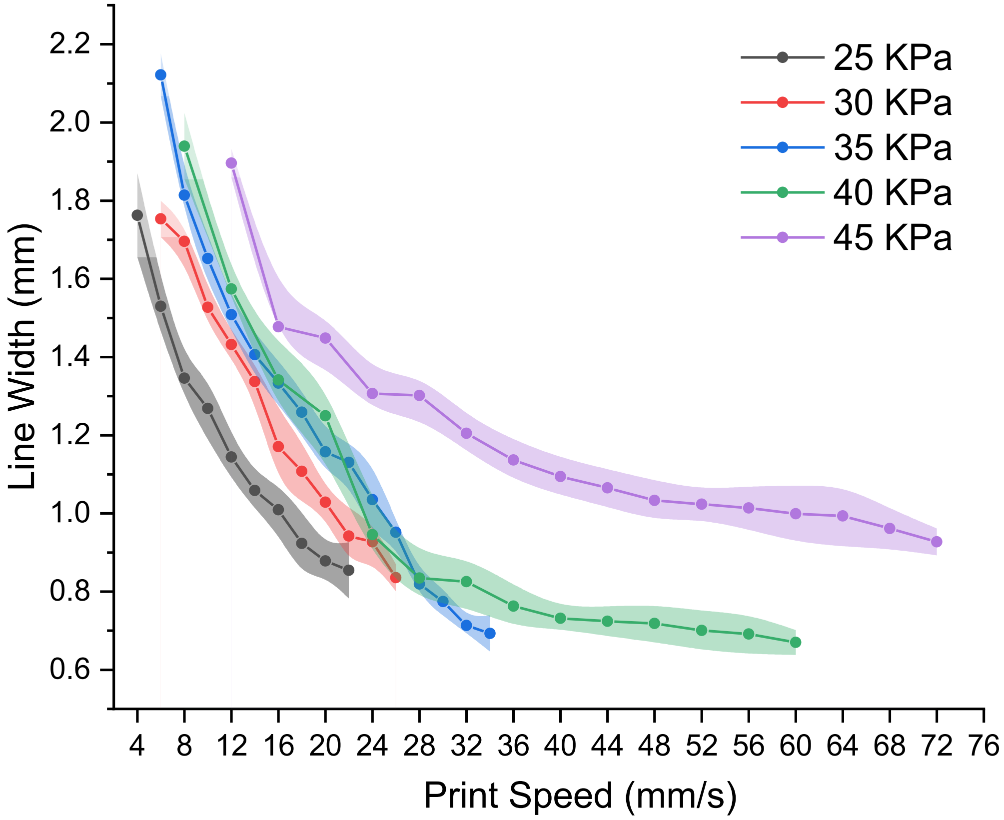

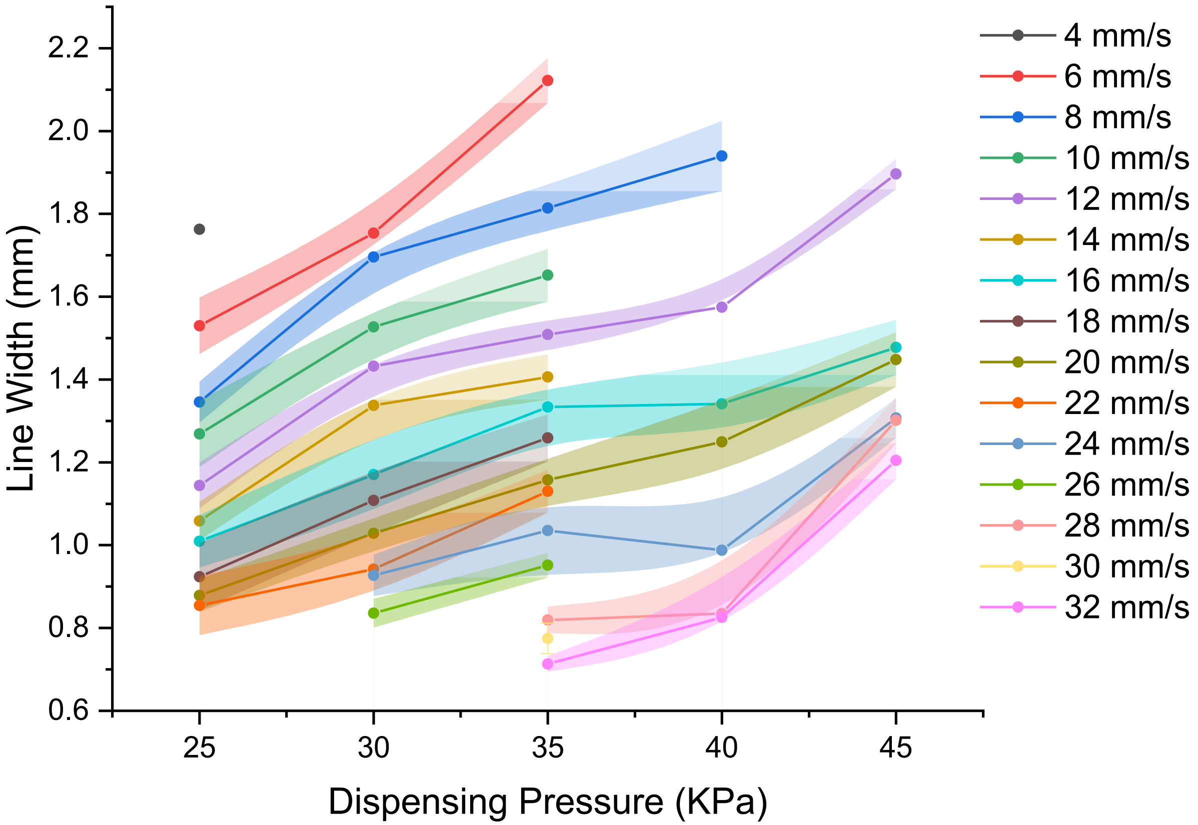

Under the same pressure, the strand width decreased **exponentially** with increasing printing speed.

At the same printing speed, the strand width increased **linearly** with increasing dispensing pressure.

3D Printing Parameter Optimization – **27G nozzle (D200um)**

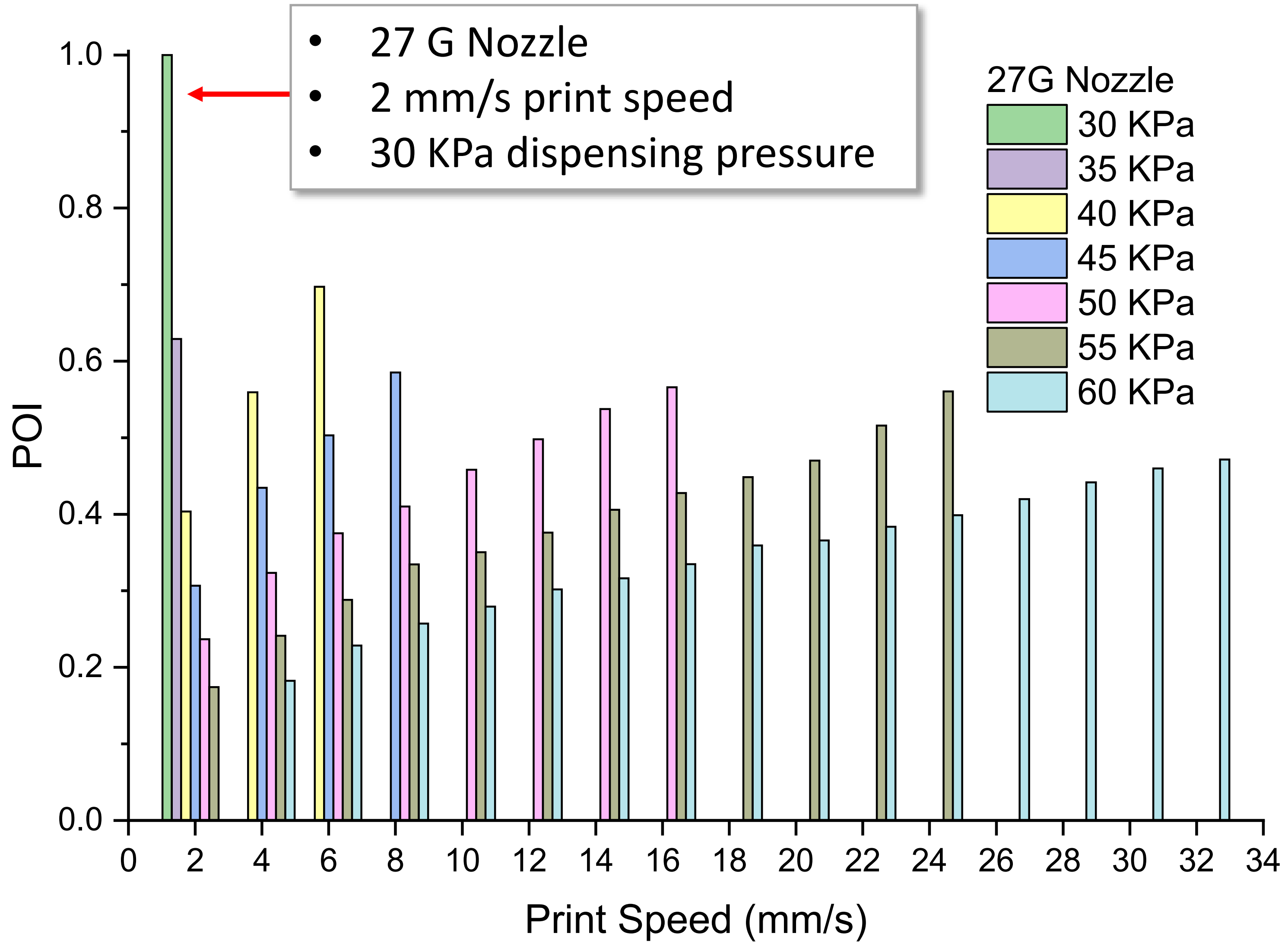

3D Printing Parameter Optimization – **22G nozzle (D410um)**

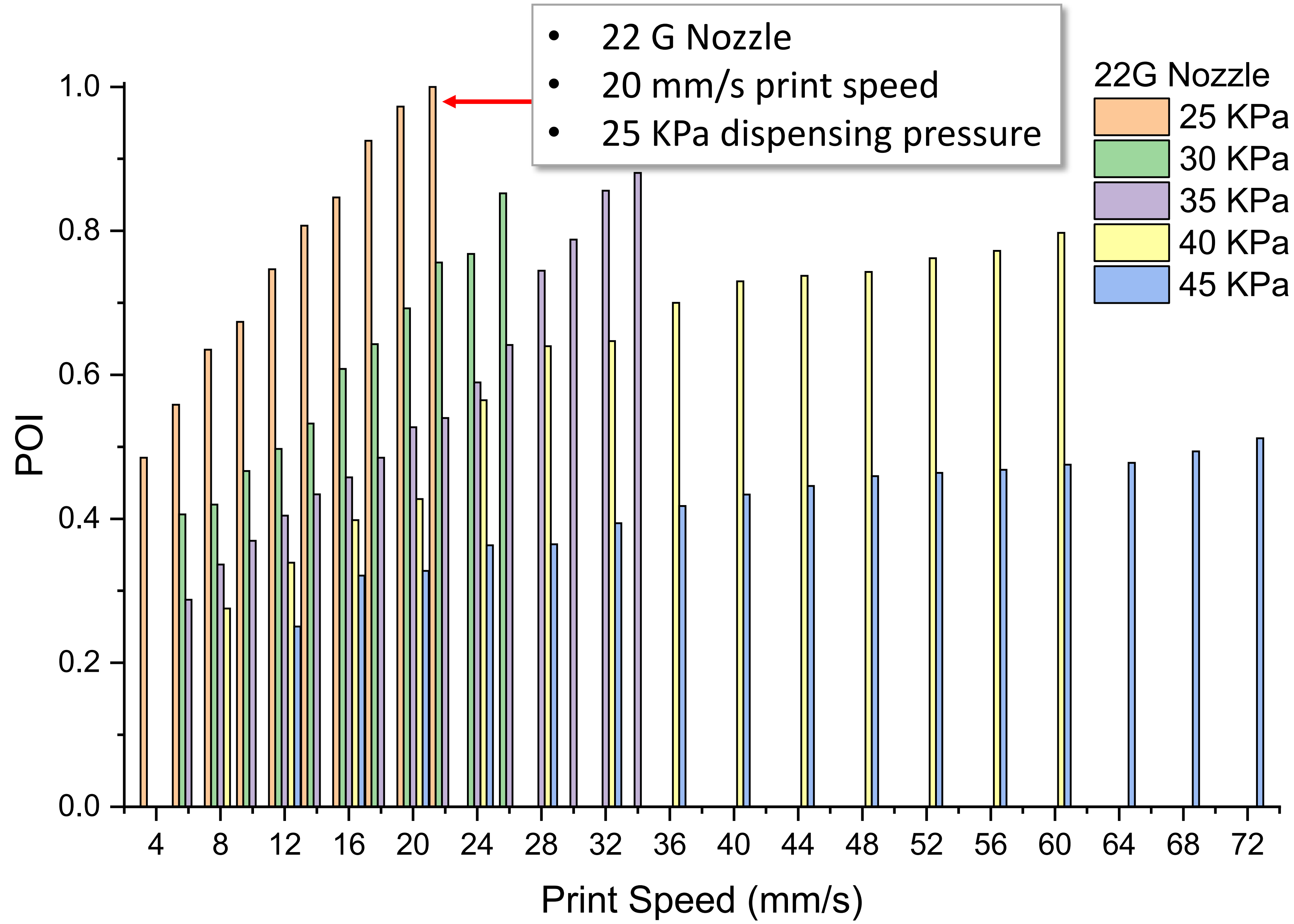

Evaluation of 2D printability by printability index

The circularity of an enclosed area: $C = \frac{4\pi A}{L^2}$, where L is the perimeter and A is the area.

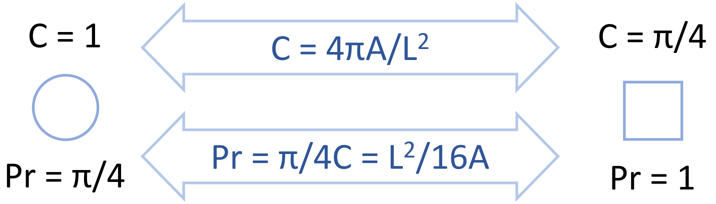

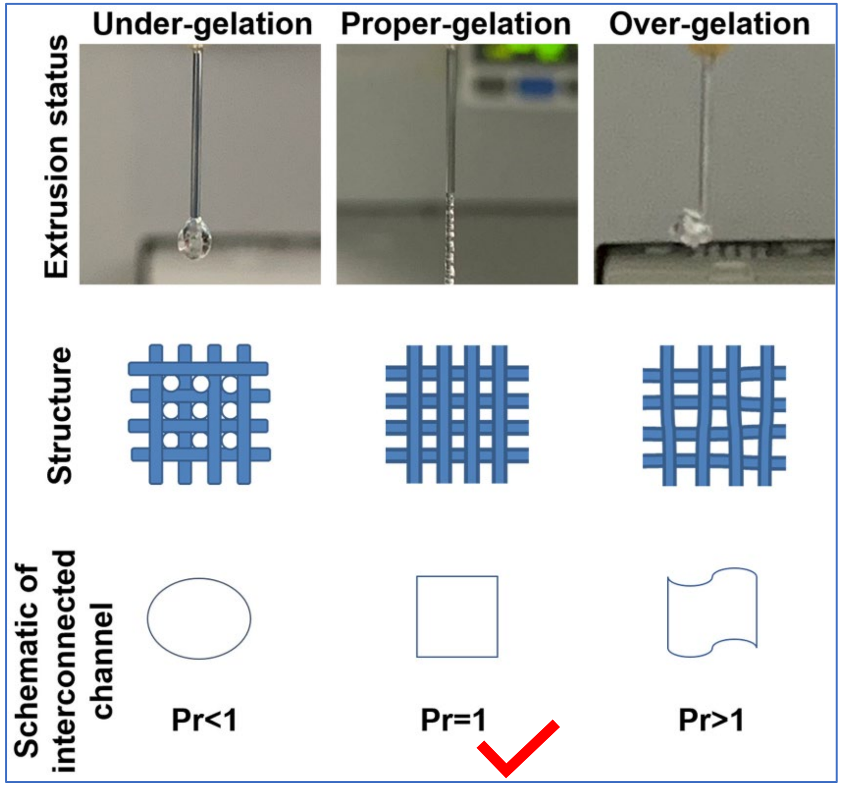

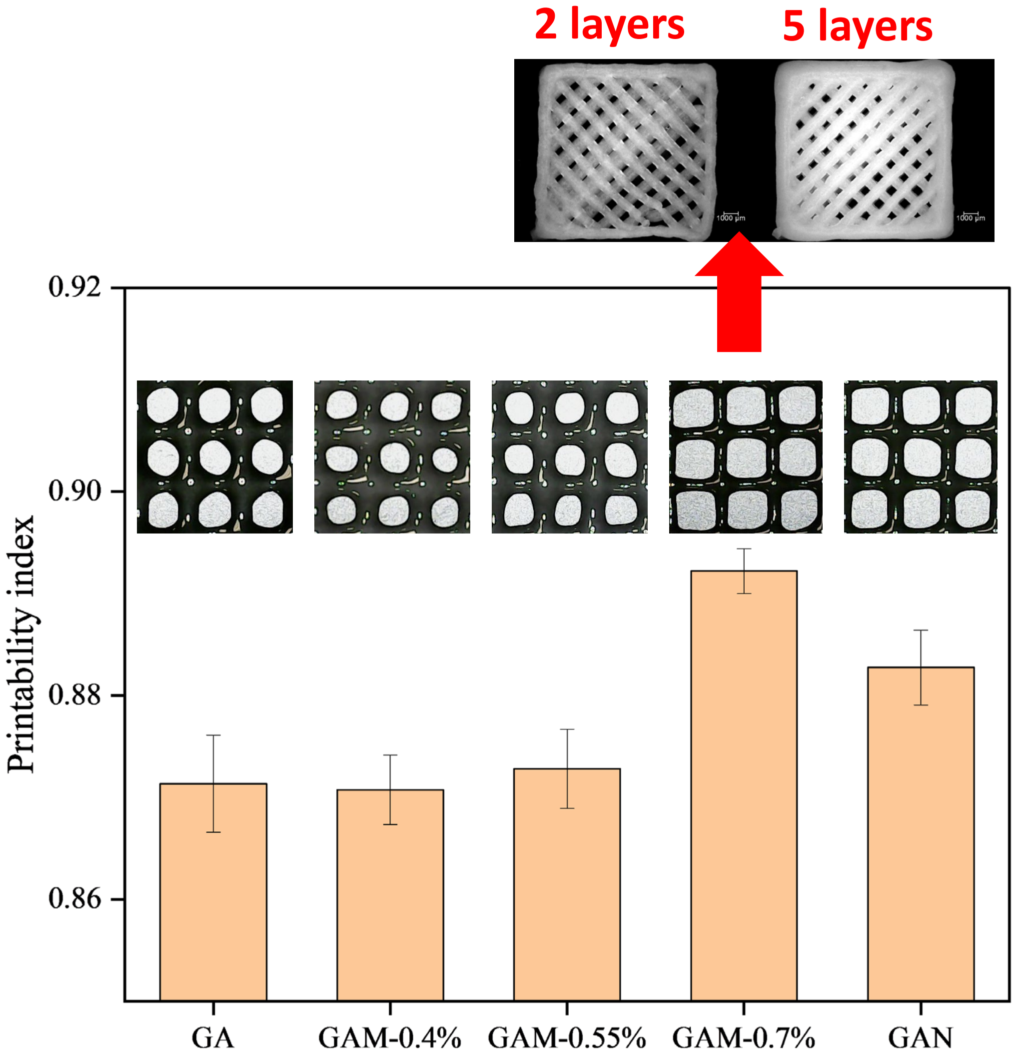

https://doi.org/10.1016/j.jmst.2022.07.011

Mechanical properties of hydrogels discs

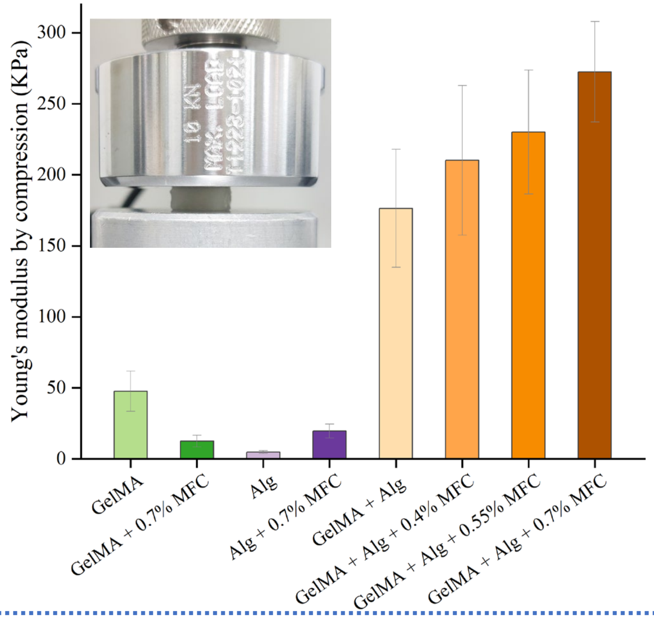

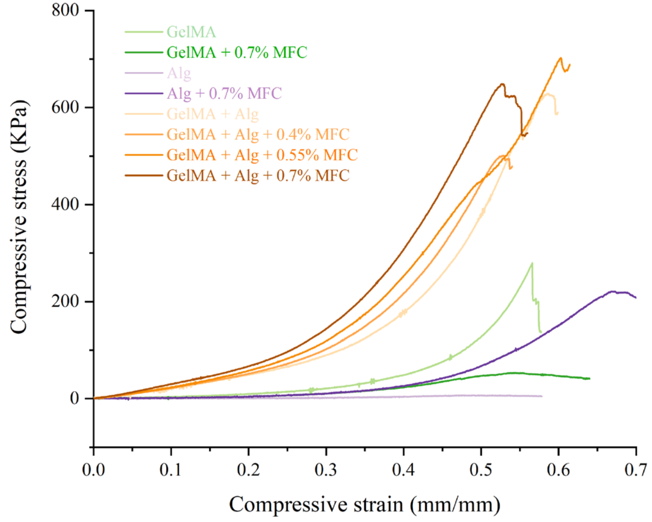

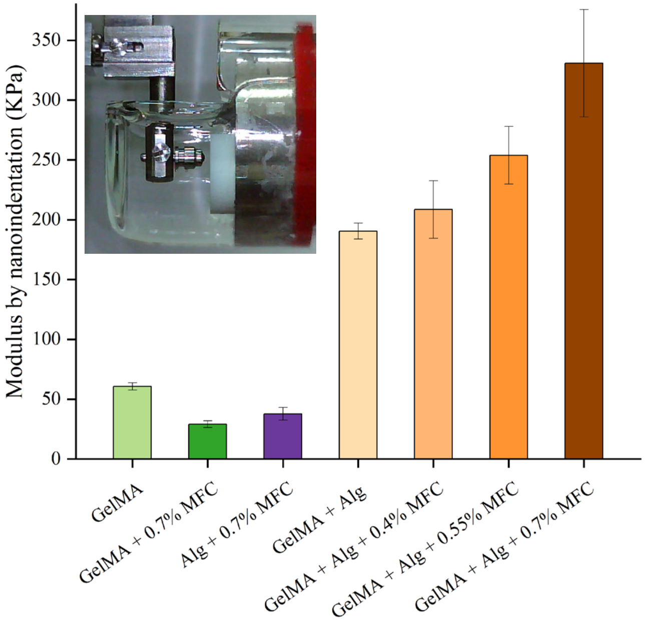

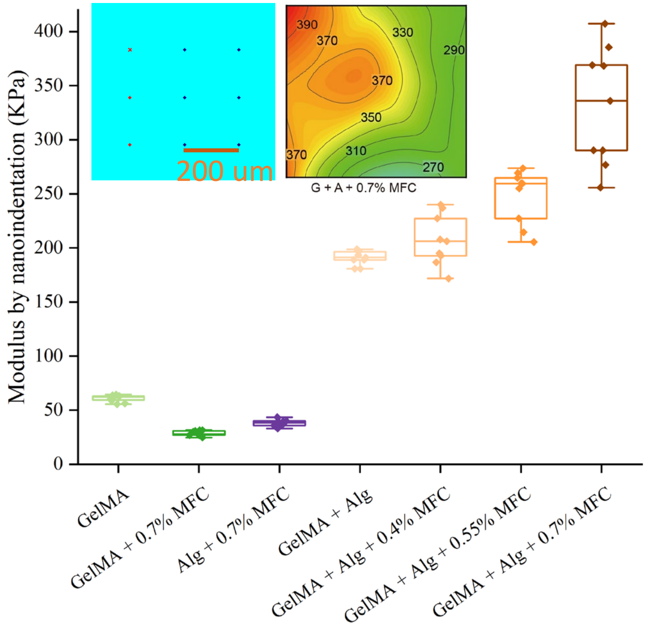

- Macro-compression and micro-indentation yielded consistent results.
- ICE network (GelMA + Alg) significantly improved the Young's modulus of the hydrogel.
- The Young's modulus further increased after MFC incorporation.
- MFC broadened the modulus distribution.
- Modulus distribution was shown by indentation test

Mechanism of mechanical reinforcement of hydrogels by study on morphology and porosity

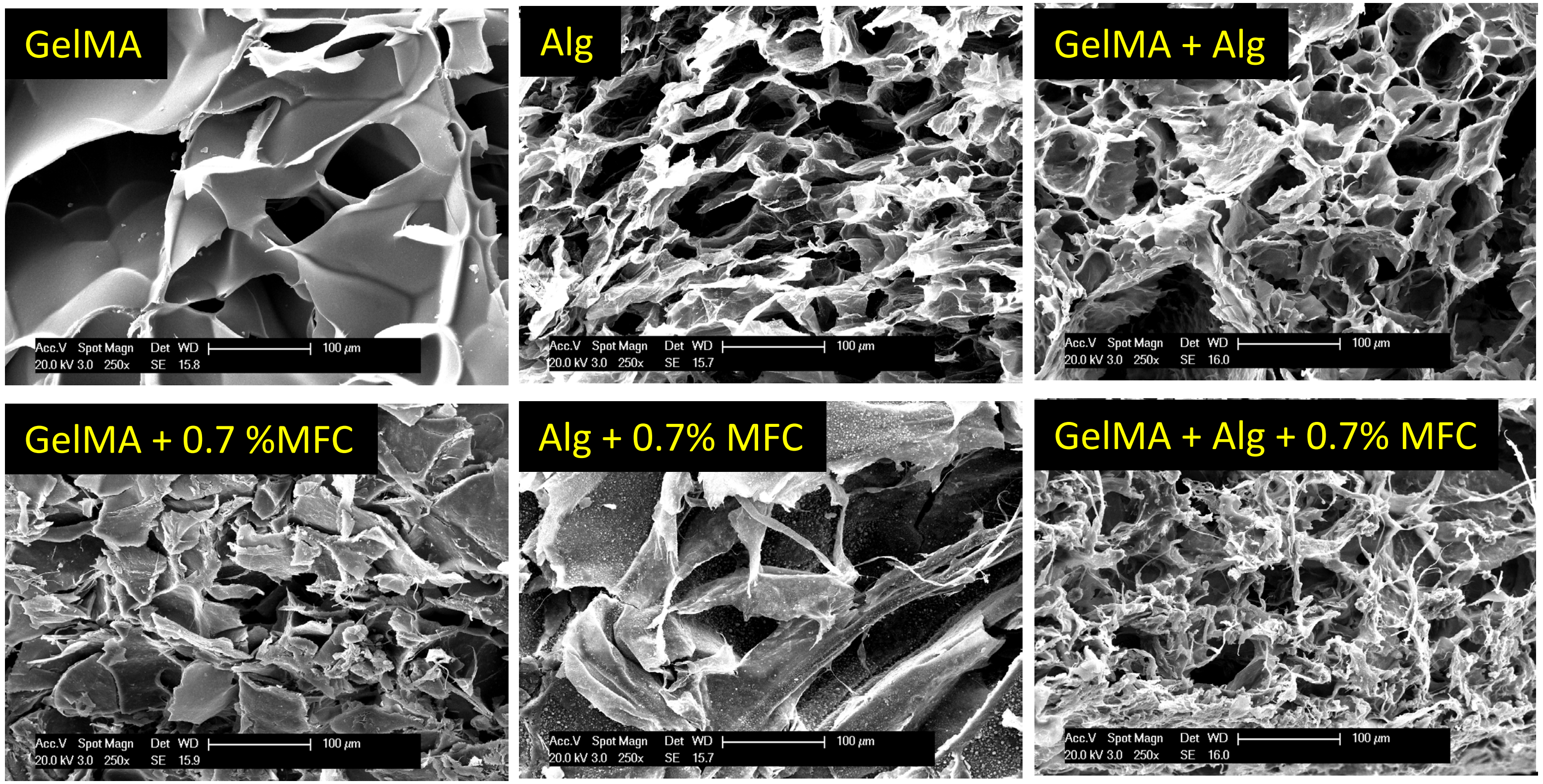

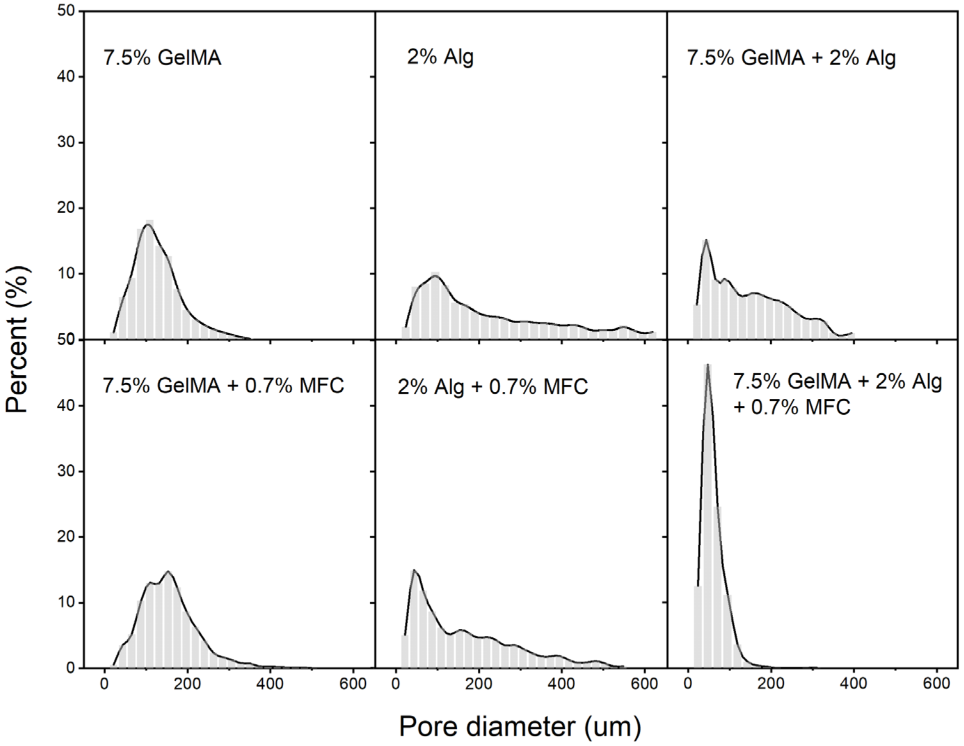

After the addition of MFC to ICE network:

- The pore size distribution became narrower;
- The average pore size decreased.

Enhancement of the mechanical strength of the hydrogel

Biocompatibility of MFC-based bioinks

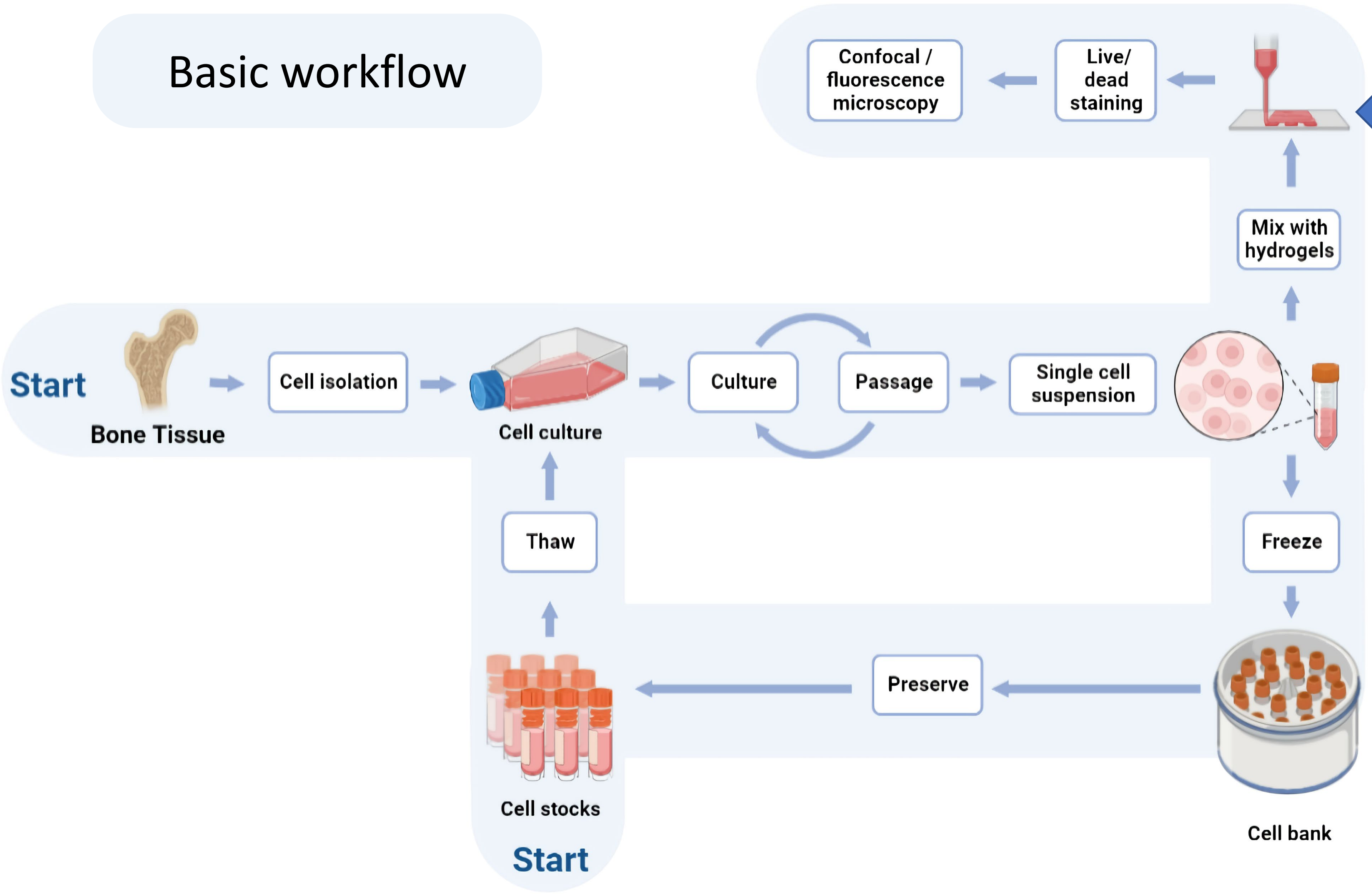

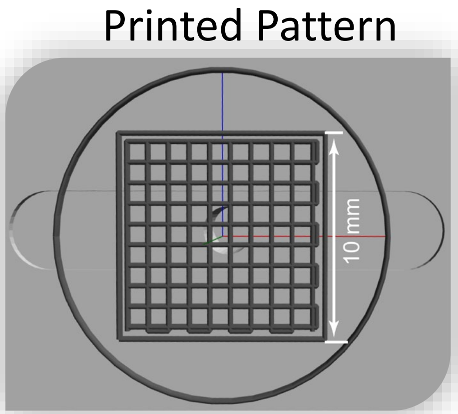

Cell number in final bioinks: 2.6×10^5 /ml

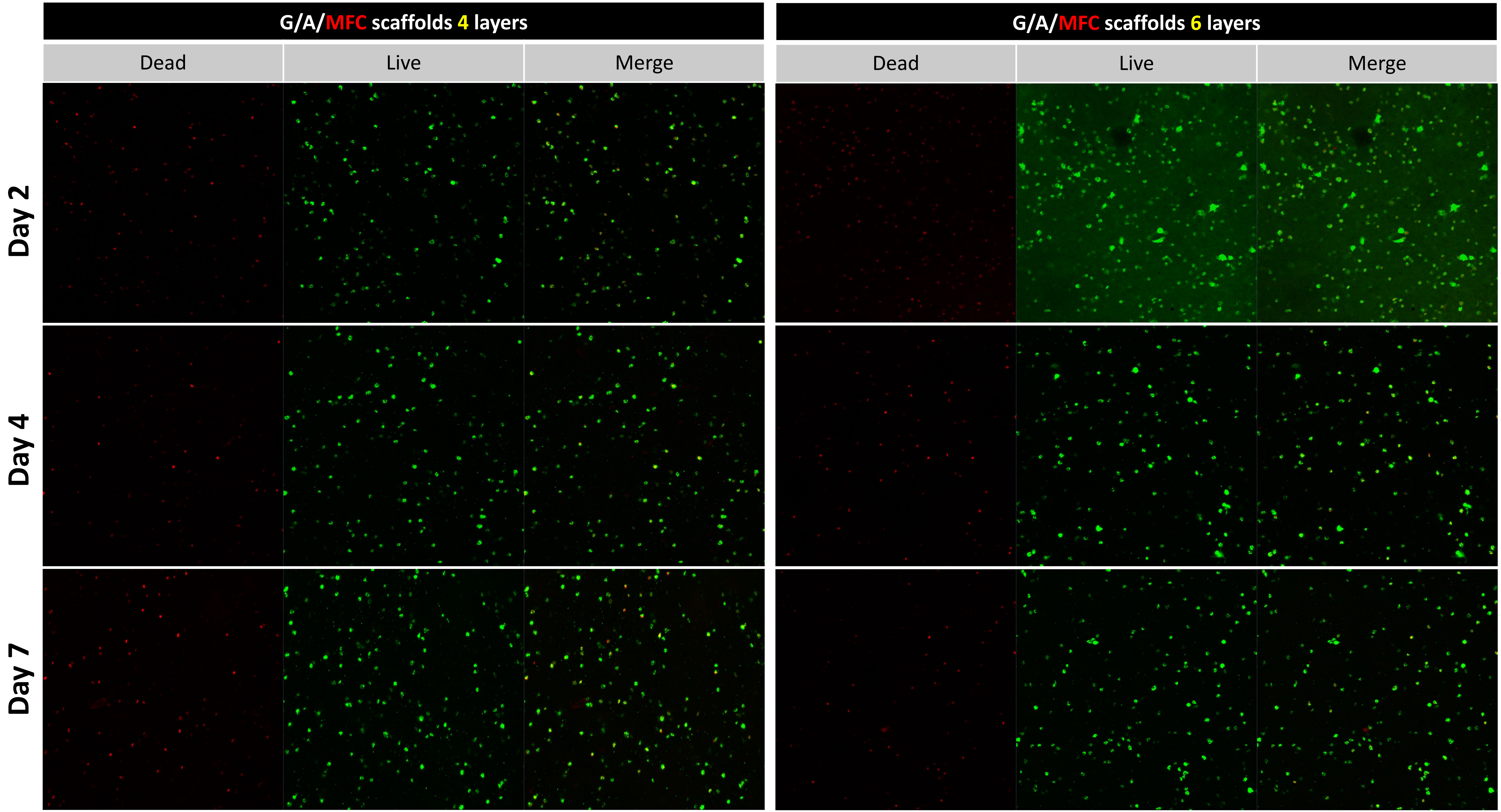
G/A/MFC scaffolds 4 layers
G/A/MFC scaffolds 6 layers
Dead
Live
Merge
Dead
Live
Merge
Day 2
Day 4
Day 7

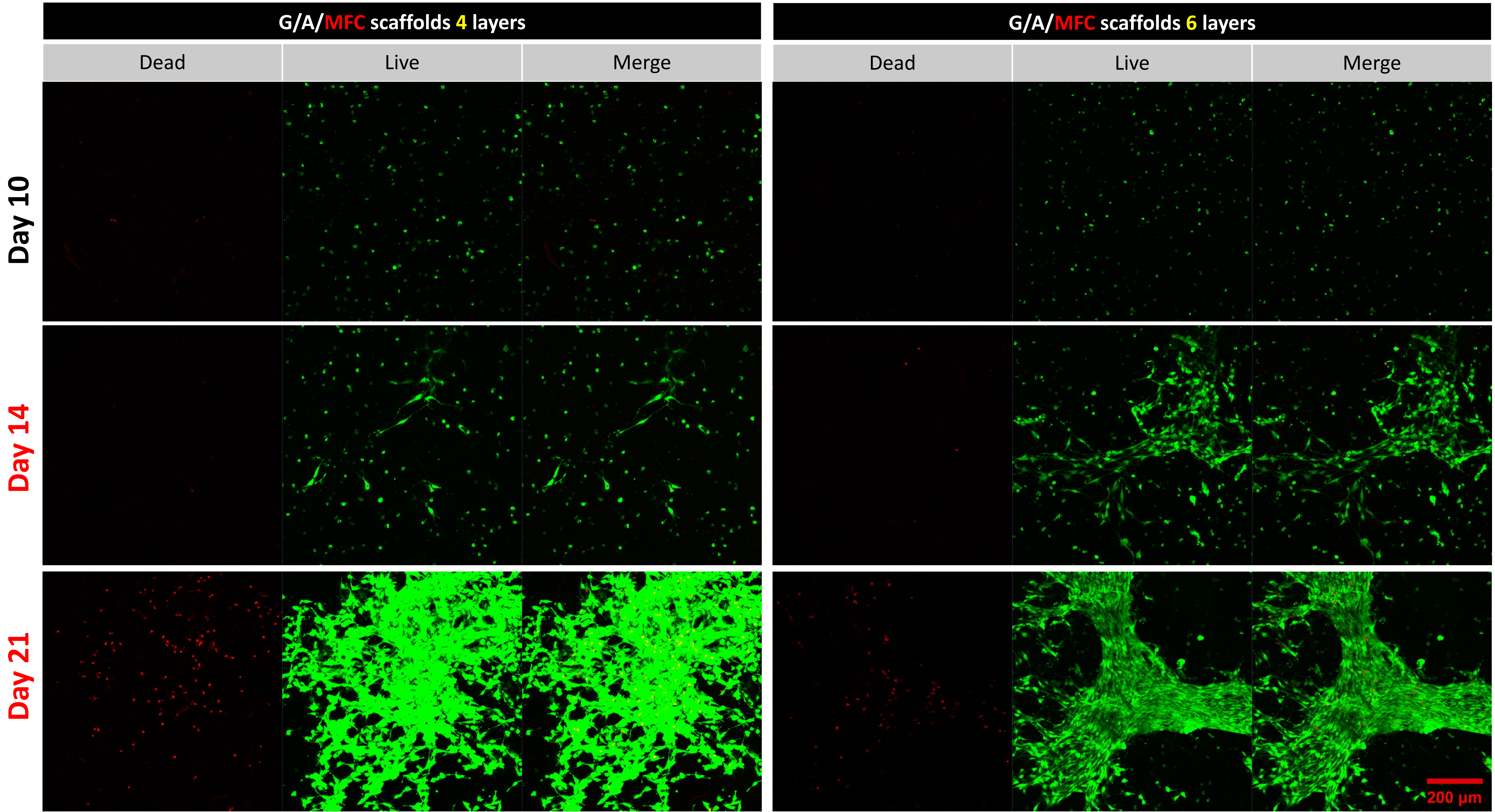

G/A/MFC scaffolds 4 layers
G/A/MFC scaffolds 6 layers
Dead
Live
Merge
Dead
Live
Merge
Day 10
Day 14
Day 21
200 μm

Conclusions

1. The incorporation of MFC in Alginate/GelMA bioink improved the rheological properties of samples, like yielding (237 Pa), shear-shinning properties (n of 0.26) and recoverability, predicting an excellent printability of the material.
2. The optimum printing conditions for the printability bioink formulation were determined and the printability of the material was assessed by the printability index.
3. The excellent mechanical properties of MFC-based ICE hydrogels (331 KPa by nanoindentation) were attributed to the synergistic effect of the ionic covalent entanglement network and the MFC porous network, as the pore size distribution of the material was significantly narrower.
4. Cells encapsulated in the hydrogels started to divide after 2 weeks of in vitro incubation and remained high viability, illustrating the biocompatibility of the bioink or hydrogel.